# System-Level Modeling and Design of Microfluidic Concentration Gradient Generators

Yi Wang[1], Tamal Mukherjee[2], Qiao Lin[3, *]

[1]*CFD Research Corporation, U.S.A.*
[2]*Department of Electrical and Computer Engineering, Carnegie Mellon University, U.S.A.*
[3]*Department of Mechanical Engineering, Columbia University, U.S.A.*

***Abstract*—This paper presents a systematic modeling and design methodology for microfluidic concentration gradient generators. The generator is decomposed into a system of microfluidic elements with relatively simple geometries. Parameterized models for such elements are analytically developed and hold for general sample concentration profiles and arbitrary flow ratios at the element inlet, hence they are valid for concentration gradient generators that rely on both complete and partial mixing. The element models are then linked through an appropriate set of parameters embedded at the element interfaces to construct a lumped-parameter and systematic representation of the entire generator network. The system model is verified by numerical analysis and experimental data and accurately captures the overall effects of network topologies, element sizes, flow rates and reservoir sample concentrations on the generation of sample concentration gradient. Finally, this modeling methodology is applied to propose a novel and compact microfluidic device that is able to create concentration gradients of complex shapes by juxtaposing simple constituent profiles along the channel width.**

***Keywords-concentration gradient generator; modeling; microfluidics; mixing***

## I. INTRODUCTION

Concentration gradients and concentration arrays of diffusible samples play important roles in the study of cell biology, biochemistry, and microfabrication [1-3]. Conventionally, the Boyden chamber, pipette, gel or their derivatives are mainly used to release the sample and investigate cell behavior subjected to the concentration gradient. However, these techniques are not effective in generating spatially stable gradients of complex shapes due to the unbalanced sample flux into and from the region of interest [2]. Therefore, a technique to generate and maintain predictable complex gradients of the sample concentration over a long period of time that can be employed to examine the correlation between sample gradients and cell behavior is strongly desired. In addition, development of sample concentration arrays also enables the high-throughout assays (e.g., immunoassay and enzyme assay) and efficient multi-dimensional screens for combinational chemistry [4, 5].

Recently laminar diffusion-based microfluidic networks have been extensively studied for the concentration-related analysis since they allow accurate and reproducible manipulation of the locations and quantities of samples released into the system. In general, these devices can be classified into two categories: complete mixing- and partial mixing-based. Complete mixing devices generally involve serially recombining, mixing, and splitting the sample solution and buffer (or sample with different concentration). Dertinger *et al.* [2] and Jeon *et al.* [3] proposed a tree-like microfluidic network to generate concentration gradients of complex shapes (e.g., linear, parabolic and periodic) along the channel width. Sample mixing before each splitting needs to be effectively complete (uniform concentration along the channel width) to allow use of design models that represent channels and sample flow rates as resistors and electrical currents in an electrical analogy. The approach was later employed in pressure driven flow [5] to perform high-throughput fluorescent immunoassays and quantitatively analyze multiple antibodies. More recently, Walker *et al.* [1] studied the effects of flow and diffusion on chemotaxis in such devices using a simplified numerical model as well as experiments. Nevertheless, to ensure the transversely complete sample mixing before each splitting, such gradient generators [2, 3] often use either bulky network configurations that are prone to leakage and clogging, or chaotic advective mixers [6] that are laborious in layout and fabrication. Additionally, profiles produced at the output channel are also discontinuous (non-smooth). Concentration gradient or array generators fully relying on diffusion-based partial mixing are simple in design and fabrication. Holden *et al.* [4] reported a Y-shape laminar microfluidic diffusion diluter (mDD) that took advantage of lateral mixing of different samples to generate transverse concentration gradients. Walker *et al.* [7] designed a cross-mixing microfluidic device that created a transverse bell-shaped concentration profile of a virus to study the cell infection within a microscale environment. While these devices are effective in generating relatively simple gradients (e.g., approximately linear or bell shaped), they have not been adequately studied for generating complex profiles (such as saw-tooth or bell-shape in [2, 8]). This is primarily due to a lack of effective models to accurately analyze the variation of sample concentration profiles in the network.

To address this issue, this paper proposes a systematic modeling approach for efficient design of both complete and partial mixing-based concentration gradient generators. In our approach, a complex generator is geometrically decomposed into a set of simple elements. Analytical models for individual elements are derived to accurately capture the dependence of fluid and sample transport on device topologies, element sizes, material properties and initial reservoir sample concentrations. Proper parameters are embedded at inlets and outlets of these element models to pass flow and concentration information between adjacent elements. As a result, the network of gradient generators can be represented as a system model by linking the

*This project was sponsored by DARPA and Air Force Research Laboratory, Air Force Material Command, USAF (Grant No. F30602-01-2-0587), and the US NSF ITR program (Award No. CCR-0325344).*

**Contact author: **ql2134@columbia.edu.***

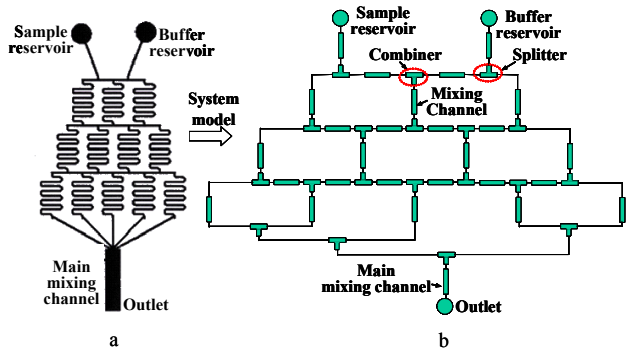


Figure 1. (a) Sketch of a tree-like gradient generator. (b) Schematic for the systematic representation of the generator.

individual elements [9]. The modeling results are validated using experimental data extracted from the literature [1] as well as full numerical analysis. To demonstrate its utility, this approach is used to propose a novel and compact microfluidic device that is capable of generating transversely complex (e.g., saw-tooth-shaped, multiple bell-shaped) concentration profiles.

## II. Systematic Representation

Our systematic approach can be illustrated with a tree-like device that consists of reservoirs, channels and intersections (Fig. 1a) and produces linear concentration profiles [1, 8]. The sample and buffer are released from their individual reservoirs, mixed as they traverse the device, and finally enter the outlet. We represent the device as a collection of interconnected mixing elements (Fig. 1b), including mixing channels, combiners (each with two input and one output streams), splitters (each with one input and two output streams), and reservoirs. Note that the multi-input intersection at the inlet of the main channel is modeled as a cascade concatenation of combiners. Then a system model can be constructed from the element models, which are assembled in correspondence to the device topology. An appropriate set of parameters (called interface parameters) are embedded at the element interfaces to enable communication of flow and concentration information between adjacent elements. As all element models are parameterized and reusable, the user can quickly compose and modify the device design in an efficient top-down manner [9].

## III. Modeling of Concentration Gradient Generators

In this section, we will first present models for the constituent elements in our systematic representation for concentration gradient generators. These element models will then be integrated for efficient, accurate and systematic evaluation of generator designs.

### *A. Element Models*

We develop models for mixing channels and combiners, which are characterized by pressure-driven laminar flow and molecular diffusion-based sample transport. In contrast to previous modeling efforts [2, 4], our models are general in that they predict transverse concentration profiles in generator designs based on complete and partial mixing with arbitrary flow rates and general inlet concentration profiles.

Mixing Channels. In this section, we consider analytical solutions of fluid flow and sample transport in a mixing channel. Neglecting entry regions at the channel inlet, the fluid flow is fully developed within the channel and governed by

$$\frac{\partial^2 u}{\partial y^2}+\frac{\partial^2 u}{\partial z^2}=-\frac{1}{\mu}\frac{\partial P}{\partial x} \tag{1}$$

where $x$, $y$, and $z$ are axial, widthwise and depth-wise coordinates, $\mu$ is the buffer's dynamic viscosity, $u$ is the axial flow velocity. Here, $x\in[0, L]$, $y\in[0, w]$ and $z\in[0, h]$; and $L$, $w$ and $h$ are the channel's length, width and depth, respectively. For fully developed flow, $dP/dx = \Delta P/L = \text{const.}$, where $\Delta P$ is the pressure difference applied over the channel length.

Equation (1) can be solved analytically [10] to yield the flow resistance of the channel:

$$R=\frac{\Delta P}{q}=\frac{12\beta L\eta}{w^4\left[1-\left(192\beta/\pi^5\right)\sum_{i=1,3,5\ldots}^{\infty}\tanh\left(i\pi/2\beta\right)/i^5\right]} \tag{2}$$

where $q=\int_0^h\int_0^w u\,dy\,dz$ is the buffer flow rate, and $\beta = w/h$ is the channel's aspect ratio. Equation (2) shows that in terms of fluid flow each mixing channel can be represented as a resistor. Thus, a steady-state pressure driven flow network can be treated as a network of electrical resistors, with pressures and volumetric flow rates analogous to voltages and currents. Kirchhoff's and Ohm's laws can be used to compute pressures at element terminals and flow rates through the elements.

Steady-state sample transport in a mixing channel is governed by the convection-diffusion equation $u\partial c/\partial x = D(\partial^2 c/\partial x^2 + \partial^2 c/\partial y^2 + \partial^2 c/\partial z^2)$, where $c$ is the sample concentration and $D$ is the sample's molecular diffusivity. Two assumptions are made to simplify the equation. First, we assume that the channel is flat, i.e., the aspect ratio is large $\beta >> 1$. It then can be shown [4] that for flat channels velocity profiles along the channel width is approximately uniform and sample transport is not affected by the depth-wise velocity distribution due to small diffusion times along the depth. This implies that the axial velocity $u$ in the convection-diffusion can be replaced with the cross-sectional average velocity, $U = q/wh$. In addition, depth-wise concentration variations can be ignored: i.e., $\partial^2 c/\partial z^2 \approx 0$. The second assumption is that the channel is long, i.e., $h << L$ and $w << L$), which implies that axial diffusion is also negligible (i.e., $\partial^2 c/\partial x^2 << \partial^2 c/\partial y^2$). Thus, the convection-diffusion is simplified to

$$U\,\partial c/\partial x = D\,\partial^2 c/\partial y^2 \tag{3}$$

Sample concentration profiles at the inlet and outlet can be represented as Fourier series: $c_{in}(\eta)=\sum_{n=0}^{\infty} d_n^{(in)}\cos(n\pi\eta)$ and $c_{out}(\eta)=\sum_{n=0}^{\infty} d_n^{(out)}\cos(n\pi\eta)$, where $\eta = y/w$ is the normalized transverse coordinate. Equation (3) can be solved analytically, also in Fourier series, to yield the input-output relationship for the Fourier coefficients $d_n$

$$d_n^{(out)} = d_n^{(in)} e^{-(n\pi)^2\tau} \tag{4}$$

where $\tau = L/(w\,\mathrm{Pe})$ is the dimensionless sample residence time in the channel, Pe = $Uw/D$ is the Peclet number, which is a characteristic ratio of convective and diffusive rates in sample transport. Note that $d_0^{(in)} = d_0^{(out)}$ are the average sample concentration over the channel's cross section.

Combiners. The combiner is a mixing element commonly used in gradient generators. In a combiner two incoming streams with certain sample concentration profiles are juxtaposed and emerge as a single combined stream with a generally reduced width. As its flow path lengths are negligible compared with those of the channels, such an element can be assumed to have zero physical size. Thus, a combiner can be represented as three resistors with zero fluidic resistance between each terminal and the internal node $N$ (Fig. 2):

$$R_l = R_r = R_{out} = 0 \tag{5}$$

where the subscripts $l$, $r$ and $out$ represent the left and right inlets and the outlet, respectively. Denote $d_m^{(l)}$ and $d_m^{(r)}$ ($m$ = 0, 1, 2…) the Fourier coefficients of the sample concentration profiles at the left and right inlets. They can be used to obtain the Fourier coefficients $d_n^{(out)}$ ($n$ = 0, 1, 2…) at the combiner outlet as follows [9]

$$d_n^{(out)} = \begin{cases} d_0^{(l)} s + d_0^{(r)}(1-s), & \text{if } n=0 \\ s\sum_{m=0}^{\infty,\ \text{if } m\neq ns} d_m^{(l)} \frac{f_1\sin(f_2)+f_2\sin(f_1)}{f_1 f_2} + & \\ s\sum_{m=0}^{\infty,\ \text{if } m=ns} d_m^{(l)} + (1-s)\sum_{m=0}^{\infty,\ \text{if } m=n(1-s)} (-1)^{n-m} d_m^{(r)} & \\ +\,2(-1)^n(1-s)\sum_{m=0}^{\infty,\ \text{if } m\neq n(1-s)} d_m^{(r)}\left(\frac{\cos(F_2/2)\sin(F_1/2)}{F_1}\right. & \text{if } n\geq 1 \\ \left. +\frac{\cos(F_1/2)\sin(F_2/2)}{F_2}\right), & \end{cases} \tag{6}$$

where $s = q_l/(q_l+q_r)$ is the flow ratio, which is the normalized flow rate of the left-side stream. Note that $s$ also gives the normalized position of the interface between the incoming streams. In (6), $f_1=(m-ns)\pi$, $f_2=(m+ns)\pi$, $F_1=(m+n-ns)\pi$ and $F_2=(m-n+ns)\pi$. Another commonly used element in concentration gradient generator is the splitter. It splits the incoming concentration profile and fluid flow, and can be modeled in a similar fashion as the combiner. The modeling detail is given elsewhere [9].

### B. *Systematic Modeling*

We now integrate element models to obtain a system model for simulation. The challenge is to communicate both fluid and sample transport information between neighboring element models at their interfaces (i.e., element terminals). This is accomplished by defining two sets of interface parameters at terminals of the element model. For an element $j$, we have $(P_i)^j$, the fluid pressure and $\{d_n^{(i)}\}^j$, the set of Fourier coefficients of the depth-averaged concentration profile along the channel width [9], where the index $i$ has values *in*, *out, l* or *r*, respectively, to represent the element's inlet, outlet, left and right inlets/outlets (for combiners and splitters). Parameters between two neighboring elements are set equal, i.e., $(P_{in})^{j+1} = (P_{out})^j$ and $\{d_n^{(in)}\}^{j+1} = \{d_n^{(out)}\}^j$ because of continuity requirements.

Simulation using system model involves computing both fluid flow parameters (including pressure and flow rates) and sample concentrations in the network. Given system topologies, element geometries and applied pressure (or equivalently volumetric flow rates) at reservoirs, pressures $(P_i)^j$ at the element terminals are first computed for the entire generator network by Kirchhoff's and Ohm's laws based on electrical analogy. The flow rate ($q$), average velocity and direction of the stream within each element, as well as the flow ratio at combiners and splitters are then calculated. With these results and user-input sample diffusivity $D$, Fourier coefficients $\{d_n^{(out)}\}^j$ of sample concentrations at the outlet of each element $j$ are determined from the corresponding values at the element's inlets using (4) and (6), and then assigned as an input to the inlet of the immediately downstream element $j$+1. This procedure starts from the most upstream sample reservoir.

## IV. Model Validation

Numerical Analysis. Numerical analysis is performed with the commercial finite volume method (FVM) simulation package CFD-ACE+ (ESI CFD, Inc.) and used as a baseline for validation of our system models. We invoke the CFD-

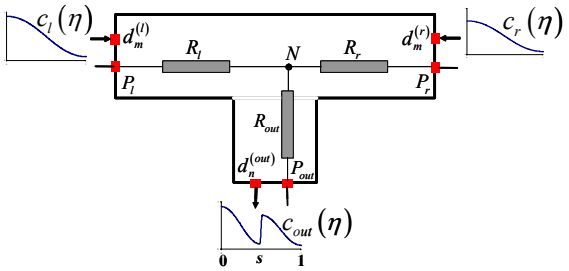


Figure 2. Modeling appraoch for the combiner.

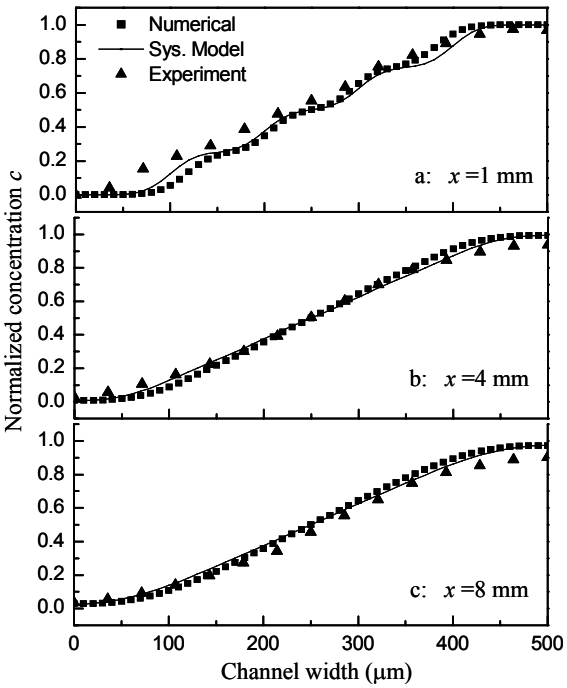


Figure 3. The systematic modeling results are compared with the numerical analysis and experimental data from the literature [1] on the evolution of an initial stepwise (five steps) profile in the main mixing channel of a tree-like gradient generator. (a) 1 mm, (b) 4 mm and (c) 8 mm downstream of the channel inlet.

ACE+ modules of incompressible fluid flow (Navier-Stokes equation) and biochemistry (convection-diffusion equation without reaction) to sequentially solve for the buffer flow velocity and sample concentration in the device. To capture the steep concentration gradient generated at physical combining and splitting junctions and mitigate numerical diffusion errors, fine meshes in the transverse direction are used. In addition, a polynomial-type mesh in the axial direction ($x$-coordinate) is selected to enable fine meshes at the junction and resolve flow entry effects on sample transport. To compare systematic modeling and numerical results, a scalar index is defined [9]:

$$M = \int_0^1 |c_N - c| d\eta \Big/ \int_0^1 c_N d\eta \qquad (7)$$

where $c$ is the normalized concentration profile from the system model and $c_N$ is the depth-averaged concentration profile from numerical analysis. Hence, $M$ represents the error of systematic modeling results relative to the numerical analysis. The smaller $M$, the better the agreement.

Experimental Validation. Our systematic modeling results are compared with experimental data reported by Walker *et al.* [1], who investigated the evolution of an initial stepwise profile in the main mixing channel (Fig. 1). The transverse concentration profile at the main channel inlet consists of five discontinuous concentration steps arising from the serial splitting, combing and mixing of the sample in the tree-like network, and is quantitatively described as: $c|_{x=0} = 0$ for $0 \le \eta \le 0.2$; $c|_{x=0} = 0.25$ for $0.2 < \eta \le 0.4$; $c|_{x=0} = 0.5$ for $0.4 < \eta \le 0.6$; $c|_{x=0} = 0.75$ for $0.6 < \eta \le 0.8$; $c|_{x=0} = 1$ for $0.8 < \eta \le 1$. Fig. 3 shows the variation of the sample (FITC-dextran) concentration profile along the main mixing channel width ($y$-coordinate) at three different axial positions ($x$-coordinate), obtained from the system model, numerical analysis as well as extracted experimental data. It can be seen that the system model agrees very well with the numerical and experimental data. The worst relative error is $M = 4.6$ % at $x = 1$ mm, which mainly occurs at channel walls and can be attributed to the associated non-uniform transverse velocity profile and the non-fully developed concentration distribution along the channel depth. The discontinuity of the initial profile (at the channel inlet) smears out due to transverse diffusion as the sample migrates down the mixing channel.

## V. Application to Concentration Gradient Generator Design

In this section, we will illustrate the utility of our systematic modeling approach by applying it to design of practically useful concentration gradient generators. Specifically, the approach is used to model a novel and compact generator that takes advantage of partial mixing. The modeling results again will be compared with the 3D numerical analysis.

Although complex concentration gradients can be generated from complete mixing [2, 3], they can be implemented with more efficient and compact partial mixing devices, which however have not been adequately explored. This is primarily because of a lack of efficient analysis tools to accurately evaluate the evolution, combining and splitting of sample concentration profiles within the mixing network. Here we propose a novel partial mixing-based generator, which is investigated with our systematic modeling method.

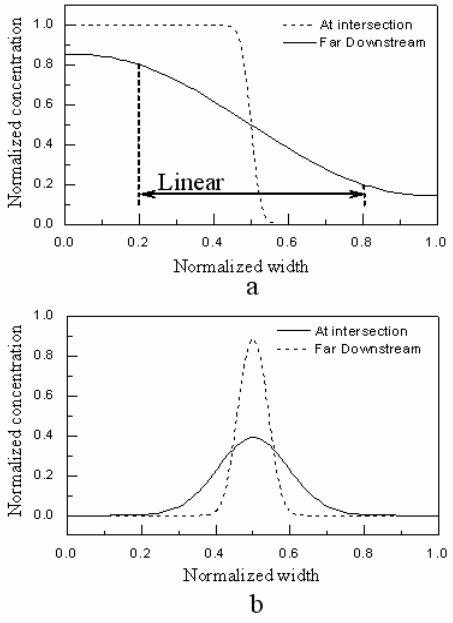


Figure 4. The transverse sample concentration profile immediately after and far downstream of the merging intersectionin. (a) a Y-mixer. (b) a cross-mixer.

Our device consists of a simple collection of Y- (or T-) and cross-mixers whose incompletely mixed concentration profiles are combined to produce desired complex gradients. In a Y-mixer, sample and buffer solvent merge at the intersection and then mix with each other in the downstream main mixing channel (Fig. 4a). The extent of sample mixing shapes the sample concentration profiles. For example, immediately after the intersection, an abrupt step-shaped profile results and the transverse position of the discontinuity is determined by sample and buffer flow rates. However, an approximately linear concentration profile forms at the far downstream, which exhibits a good linearity at the channel center (~20-80 % of the channel width). Similarly, a bell-shaped profile that has been employed in [8] to investigate neutrophil chemotaxis can be created by a cross-mixer as shown in Fig. 4b. The sample is injected from the middle channel and sandwiched by buffer solvent from side channels [9]. Inter-stream diffusion in the main mixing channel smoothes and produces sample concentration profiles with different band width and height. By juxtaposing these constituent concentration profiles, temporally and spatially stable gradients of complex shapes can be attained. As the constituent profiles are independent from each other, their shape characteristics (e.g., the width, slope, peak and mean concentration value) can be individually adjusted by choice of branch flow rates, channel sizes and reservoir sample concentrations. In the examples below, all channels have a depth of $h$ = 60 μm with an aspect ratio ($\beta$) of 5~20. The volumetric flow rate in the main mixing channel is fixed at 5.18 μl/min, corresponding to a practically relevant velocity of 1200 μm/s [1]. We use a typical sample diffusivity of $D$ = $1\times10^{-10}$ $m^2/s$, and the normalized reservoir sample concentration ranging from 0 to 1, unless otherwise noted.

Saw-tooth-shaped concentration profiles. Transverse saw-tooth-shaped concentration profiles [2] can be generated by juxtaposing multiple Y-mixing units (Fig. 5a). Sample solutions with different concentrations are released from two adjacent reservoirs in a Y-mixing unit (e.g., reservoirs 1 and 2), and then mix with each other in the serpentine mixing channel to generate an approximately linear profile. The peak and mean concentration value and the slope of the constituent profile are determined from the initial reservoir concentrations, serpentine channel sizes and flow rates that can be effectively captured by our system model (4). Eventually, the approximately linear profiles from serpentine mixing channels are combined in the main mixing channel to achieve a saw-tooth-shaped distribution. Fig. 5b demonstrates a saw-tooth shape consisting of three constituent concentration profiles, each having the same mean values but different peak values and slopes. As an extreme case, given a sufficiently fast flow velocity or a extremely short serpentine mixing channel, sample mixing in the Y-mixing unit is negligible, leading to a profile comprised of three square waves. In Fig. 5, steep concentration discontinuities are created at the interface between streams, which can be useful for studying the cell behavior subjected to abrupt gradients [8]. Excellent agreement between numerical and systematic modeling results with the worst case error $M$ = 4.8 % indicates that our model is able to accurately predict discontinuous profiles as well as their evolution along the stream direction.

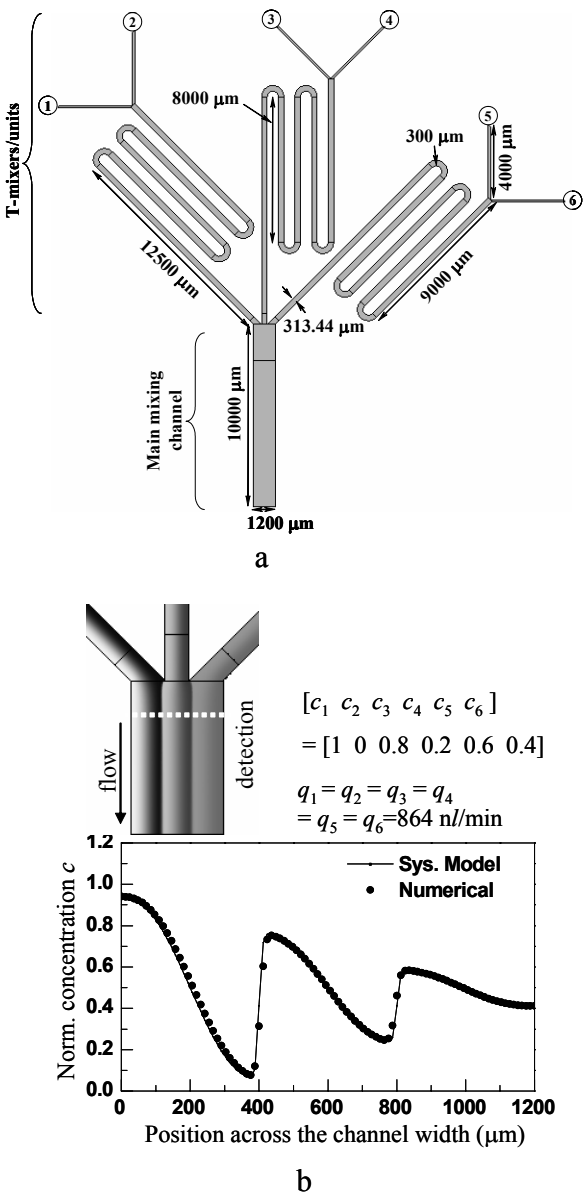


Figure 5.(a) Network topology and dimensions of a saw-tooth concentration gradient generator. (b) Numerical contour plots of the sample concentration and comparison between numerical simulation and systematic modeling results on concentration profiles across the channel width (extracted 400 μm downstream of the intersection).

Multiple-bell-shaped concentration profiles. To create a multiple-bell-shaped concentration profile, cross-mixers can be assembled laterally (Fig. 6a). Constituent bell-shaped concentration profiles first form in the cross-mixing units as described above, which then merge together in the main mixing channel to create a multiple-bell-shaped profile. Fig. 6b shows the numerical contour plot of the sample concentration as well as the comparison of the results from numerical analysis and system model. Different from that in Fig. 4b, asymmetric constituent bell-shaped profiles are generated in the cross-mixing units, which is enabled by feeding different sample concentration at reservoirs 1, 3 and 4, 6, leading to a higher sample concentration value at the centerline of the main

channel. Excellent agreement between numerical and system model results has been obtained with the relative average error $M = 4$ %.

## VI. Conclusion

A systematic modeling approach has been presented to assist the design of concentration gradient generators, in which the generator is geometrically disassembled into a collection of elements with relatively simple geometries. Analytical and parameterized models for the elements (e.g., mixing channels and combiners) in pressure driven flow have been developed to capture the overall effects of the generator geometry, material properties, and operational protocols on sample transport. These elements are then integrated, enabled by the appropriate interface parameters at element terminals, to form a system model representing the entire generator network. Modeling results exploring concentration gradient generators based on both complete and partial mixing are compared with experimental data from the literature and full numerical analysis. Excellent agreement with the worst case error $M <$ 5% has been achieved relative to numerical analysis.

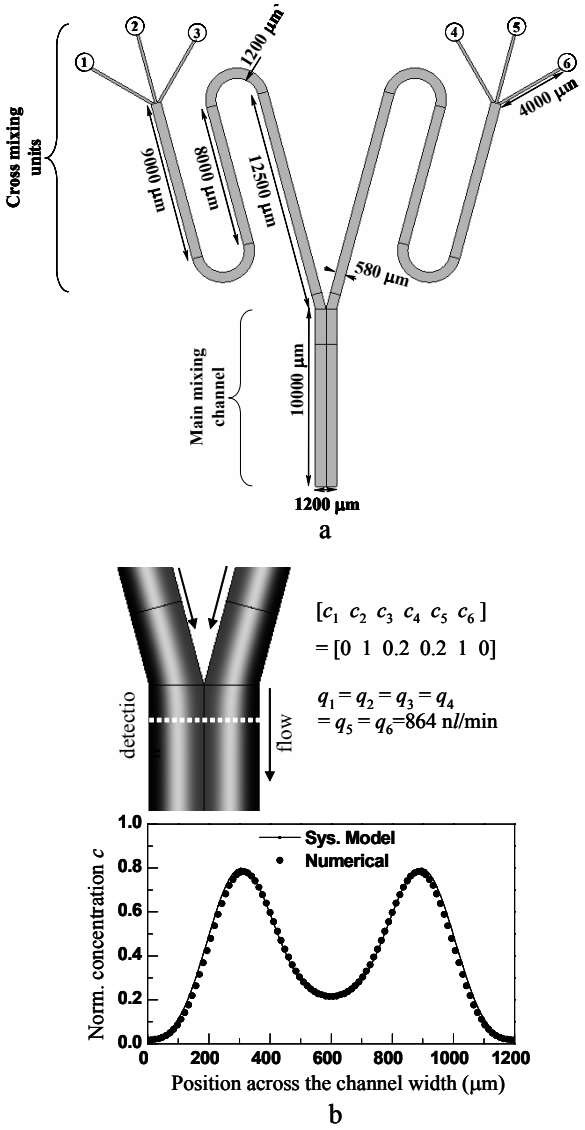


Figure 6.(a) Network topology and dimensions of a multiple-bell-shaped concentration gradient generator. (b) Numerical contour plots of the sample concentration and comparison between numerical and systematic modeling results on transverse concentration profile (extracted 400 µm downstream of the intersection).

The system model is then exploited to propose a novel generator capable of creating stable and complex concentration gradients. The main underlying principle is to juxtapose simple constituent (e.g., approximately linear and bell-shaped) profiles arising from Y- or cross-mixers to obtain composite profiles with a higher level of complexity (e.g., saw-tooth and multiple-bell shaped). The class of achievable concentration profiles (e.g., linear or bell-shaped) is determined from the type of the mixers (e.g., cross- or Y-mixers) and their spatial configurations. The constituent profile details (e.g., slope, mean and peak concentration values, position and width) are primarily dictated from the initial reservoir concentrations, flow rates, sample properties as well as the channel dimensions. This insightful observation assists selection of appropriate parameters to attain desired concentration profiles using iterative evaluation of system models.

## References


[1] G. M. Walker, J. Q. Sai, A. Richmond, M. Stremler, C. Y. Chung, and J. P. Wikswo, "Effects of flow and diffusion on chemotaxis studies in a microfabricated gradient generator," *Lab on a Chip*, vol. 5, pp. 611-618, 2005.

[2] S. K. W. Dertinger, D. T. Chiu, N. L. Jeon, and G. M. Whitesides, "Generation of gradients having complex shapes using microfluidic networks," *Analytical Chemistry*, vol. 73, pp. 1240-1246, 2001.

[3] N. L. Jeon, S. K. W. Dertinger, D. T. Chiu, I. S. Choi, A. D. Stroock, and G. M. Whitesides, "Generation of solution and surface gradients using microfluidic systems," *Langmuir*, vol. 16, pp. 8311-8316, 2000.

[4] M. A. Holden, S. Kumar, E. T. Castellana, A. Beskok, and P. S. Cremer, "Generating fixed concentration arrays in a microfluidic device," *Sensors and Actuators B-Chemical*, vol. 92, pp. 199-207, 2003.

[5] X. Y. Jiang, J. M. K. Ng, A. D. Stroock, S. K. W. Dertinger, and G. M. Whitesides, "A miniaturized, parallel, serially diluted immunoassay for analyzing multiple antigens," *Journal of the American Chemical Society*, vol. 125, pp. 5294-5295, 2003.

[6] X. Y. Jiang, Q. B. Xu, S. K. W. Dertinger, A. D. Stroock, T. M. Fu, and G. M. Whitesides, "A general method for patterning gradients of biomolecules on surfaces using microfluidic networks," *Analytical Chemistry*, vol. 77, pp. 2338-2347, 2005.

[7] G. M. Walker, M. S. Ozers, and D. J. Beebe, "Cell infection within a microfluidic device using virus gradients," *Sensors and Actuators B-Chemical*, vol. 98, pp. 347-355, 2004.

[8] N. L. Jeon, H. Baskaran, S. K. W. Dertinger, G. M. Whitesides, L. Van de Water, and M. Toner, "Neutrophil chemotaxis in linear and complex gradients of interleukin-8 formed in a microfabricated device," *Nature Biotechnology*, vol. 20, pp. 826-830, 2002.

[9] Y. Wang, Q. Lin, and T. Mukherjee, "A model for laminar diffusion-based complex electrokinetic passive micromixers," *Lab on a Chip*, vol. 5, pp. 877-887, 2005.

[10] F. M. White, *Viscous fluid flow*, 2nd ed. New York: McGraw-Hill, 1991.